Acta Crystallographica Section D
Biological Crystallography
ISSN 0907-4449

Molecular complementarity between tetracycline and the GTPase active site of elongation factor Tu

Susan E. Heffron,[a] Suet Mui,[a]† Annette Aorora,[a]§ Kenton Abel,[a]¶ Ernst Bergmann[a]‡‡ and Frances Jurnak[a,b]*

[a]Department of Physiology and Biophysics, 346-D Med Sci I, University of California, Irvine, CA 92697-4560, USA, and [b]Member, The Chao Family Comprehensive Cancer Center, University of California, Irvine, USA

† Deceased.
§ Present address: Cell Biology Laboratory, Hoag Hospital, One Hoag Drive, Newport Beach, CA 92658-6100, USA.
¶ Present address: Xencor Inc., 111 West Lemon Avenue, Monrovia, CA 91016, USA.
‡‡ Present address: Department of Biochemistry, University of Alberta, Edmonton, Alberta T6G 2H7, Canada.

Correspondence e-mail: jurnak@uci.edu

Received 6 April 2006
Accepted 2 September 2006

PDB References: tetracycline–EF-Tu complexes, $P2_1$ form, 2hdn, r2hdnsf; $P4_32_12$ form, 2hcj, r2hcjsf.

Two crystal forms of a complex between trypsin-modified elongation factor Tu–MgGDP from *Escherichia coli* and the antibiotic tetracycline have been solved by X-ray diffraction analysis to resolutions of 2.8 and 2.1 Å, respectively. In the $P2_1$ form, cocrystals were grown from a solution mixture of the protein and tetracycline. Six copies of the trypsin-modified EF-Tu–MgGDP–tetracycline complex are arranged as three sets of dimers in the asymmetric unit. In the second crystal form, tetracycline was diffused into $P4_32_12$ crystals, resulting in a monomeric complex in the asymmetric unit. Atomic coordinates have been refined to crystallographic R factors of 18.0% for the $P2_1$ form and 20.0% for the $P4_32_12$ form. In both complexes, tetracycline makes significant interactions with the GTPase active site of EF-Tu. The phenoldiketone moiety of tetracycline interacts directly with the Mg^{2+}, the α-phosphate group of GDP and two amino acids, Thr25 and Asp80, which are conserved in the GX_4GKS/T and DX_2G sequence motifs found in all GTPases and many ATPases. The molecular complementarity, previously unrecognized between invariant groups present in all GTPase/ATPases and the active moiety of tetracycline, may have wide-ranging implications for all drugs containing the phenoldiketone moiety as well as for the design of new compounds targeted against a broad range of GTPases or ATPases.

1. Introduction

Tetracycline is a broad-spectrum antibiotic which inhibits bacterial ribosomal function. Tetracycline is widely believed to prevent the binding of aminoacyl-tRNA to the A site of mRNA-programmed ribosomes (Schnappinger & Hillen, 1996; Chopra & Roberts, 2001). The bacteriostatic mode of action of tetracycline has been extensively studied over the last 50 years and it is well established that the pharmacologically active region is the phenoldiketone moiety highlighted in Fig. 1 (Brown & Ireland, 1978; Rogalski, 1985). The primary molecular target of tetracycline binding is believed to be the ribosome. Initially, one or more ribosomal proteins had been implicated (Connamacher & Mandel, 1968; Maxwell, 1968), but in recent years ribosomal RNA has become the favored binding site. With association constants in the range of 3.0×10^5 M, tetracycline exhibits weak affinity for multiple sites on *Escherichia coli* ribosomes (Epe & Woolley, 1984). A single site with a tenfold stronger affinity for tetracycline has been found on the *E. coli* S7 ribosomal protein of the 30S subunit (Goldman *et al.*, 1983; Buck & Cooperman, 1990).

The focus on rRNA as a possible binding site began when tetracycline was shown to alter the normal dimethylsulfate modification of three sites on *E. coli* 16S rRNA (Moazed & Noller, 1987). Additional studies confirmed an interaction

between 16S RNA and tetracycline (Oehler *et al.*, 1997; Noah *et al.*, 1999). Subsequently, two structural studies in which tetracycline was diffused into pregrown crystals of the 30S ribosomal subunit identified several sites in which tetracycline made direct contacts with rRNA (Brodersen *et al.*, 2000; Pioletti *et al.*, 2001). Two of the tetracycline-binding sites were similar in both structures. In the highest occupancy site, tetracycline primarily formed interactions with the H34 region of 16S RNA implicated in binding to aminoacyl-tRNA, thus increasing speculation that this site was the primary target of tetracycline inhibition. Tetracycline also interacted with the sugar-phosphate backbone in H34 *via* an Mg^{2+} ion, in a fashion similar to the tetracycline repressor–Mg–tetracycline complex (Hinrichs *et al.*, 1994; Orth *et al.*, 1999). The second shared tetracycline-binding site is located in the body of the 30S subunit, sandwiched between H27 and the top of H11 in the 5′ domain of 16S RNA. Unlike the primary site, the 16S RNA mediates all interactions with the tetracycline in the absence of an Mg^{2+} ion.

Despite the common assumption that the ribosome was the primary target of tetracycline action, the definitive proof, a site-specific mutation which rendered the ribosome resistant to tetracycline, eluded investigators for many years. Prior to 1998, there was only a single unconfirmed report of a mutant ribosomal protein, S10, which conferred tetracycline resistance upon one bacterial type, *Bacillus subtilis* (Williams & Smith, 1979). In 1998, a G1058C mutation in 16S RNA was identified in clinical isolates of cutaneous propionibacteria resistant to tetracycline (Ross *et al.*, 1998). Although the G1058C mutation was not found in laboratory mutants of other bacteria, the mutant was recreated by site-directed mutagenesis of cloned *E. coli* ribosomes. *E. coli* strains carrying the mutant plasmids were more resistant to tetracycline than wild-type plasmids. In subsequent years, 16S RNA mutations in the H31 region which conferred tetracycline resistance were found, but only in clinical isolates of *Helicobacter pylori* (Nonaka *et al.*, 2005, and references therein). In other bacterial pathogens, more complex mechanisms of resistance had evolved, including efflux mechanisms, the emergence of proteins that catalyze the dissociation of tetracycline from the ribosome and mechanisms involving enzymatic inactivation of the drug. The predominance of complex resistance mechanisms in nature, rather than a simple 16S RNA mutation to prevent tetracycline binding, raises the question as to whether or not there is more than one mode of tetracycline inhibition and if the inhibition mechanisms are the same in all bacterial pathogens.

Early reports (Gordon, 1969; Lucas-Lenard *et al.*, 1969; Ravel *et al.*, 1969; Shorey *et al.*, 1969; Skoultchi *et al.*, 1970; Spirin *et al.*, 1976; Semenkov *et al.*, 1982) that elongation factor Tu (EF-Tu) might play a role in tetracycline inhibition were routinely dismissed because the antibiotic disrupts *in vitro* ribosomal assays under non-enzymatic conditions. Overlooked in all discussions were the differing experimental conditions of the *in vitro* ribosomal assays and any effect that this might have upon the results. The possibility that EF-Tu might be one of several tetracycline targets was raised anew when tetracycline was reported to crystallize as a 1:1 complex with the trypsin-modified form of *E. coli* EF-Tu–MgGDP (tm-EF-Tu–MgGDP; Mui *et al.*, 1990). The structure of the complex is reported here and is compared with the structure of a tm-EF-Tu–MgGDP–tetracycline complex which was formed by diffusion of tetracycline into preformed $P4_32_12$ crystals of tm-EF-Tu–MgGDP. The results demonstrate that tetracycline not only binds to tm-EF-Tu–MgGDP, but does so by interacting with an important structural motif that is shared by all GTPases and many ATPases. The results have far-ranging implications that will be discussed.

2. Experimental methods

2.1. $P2_1$ crystal form

2.1.1. Crystallization, data collection, data processing and heavy-atom phasing. Crystals of the trypsin-modified EF-Tu–MgGDP–tetracycline complex were grown as previously described (Mui *et al.*, 1990). The cocrystals belong to space group $P2_1$, with unit-cell parameters a = 69.71, b = 156.06, c = 134.83 Å, β = 95.38° and six complex molecules per asymmetric unit. Two derivatives, methylmercury acetate and

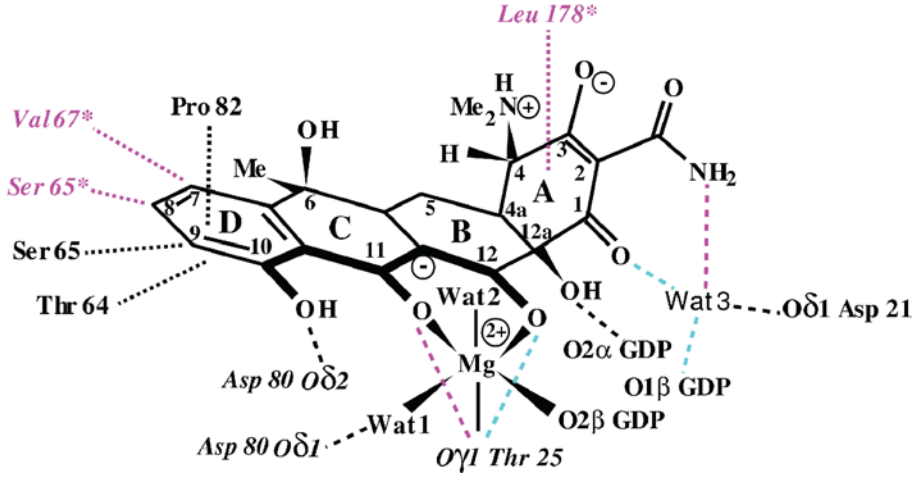

Figure 1
Chemical structure of the polar zwitterionic form of tetracycline and schematic description of the interactions between tm-EF-Tu–MgGDP and tetracycline. The active phenoldiketone moiety is highlighted in bold and the atoms are labeled according to the standard nomenclature for tetracycline. Interactions which are observed in both the $P2_1$ and $P4_32_12$ forms are shown in black. Those interactions that are only found in the $P2_1$ form are shown in pink and those interactions found only in the $P4_32_12$ form are shown in blue. The lines with longer dashes indicate hydrogen bonds and the lines with shorter dashes indicate hydrophobic interactions. Wat 1 and Wat 2 are water ligands in the octahedral coordination shell of Mg^{2+} and Wat 3 is a water molecule that interacts directly with tetracycline.

Table 1
Data statistics for native and derivatives.

	$P2_1$			$P4_32_12$
	Native	Hg	Pb	Native
Resolution (Å)	2.7	2.7	2.7	2.1
No. reflections measured	432153	236803	159967	56433
No. of unique reflections	73085	68431	68735	20748
Completeness (%)	92.3	86.1	87.6	92.5
No. of crystals	6	3	2	1
$I/\sigma(I)$	11.9	8.0	11.3	11.1
$R_{\rm merge}$† (%)	9.9	11.3	6.3	4.6
$R_{\rm scale}$‡	—	19.1	27.7	—
$R_{\rm Cullis}$§	—	0.56	0.73	—
$F_{\rm H}/E$¶	—	1.18	0.61	—

† $R_{\rm merge} = 100 \times \sum |(I_{\rm avg} - I_{\rm obs})| / \sum I_{\rm avg}$, where I is the average (avg) or the observed (obs) intensity of the reflection. ‡ $R_{\rm scale} = 100 \times \sum \big||F_{\rm nat}| - |F_{\rm der}|\big| / \sum (F_{\rm nat} + F_{\rm der})$, where F is the native (nat) or the derivative (der) structure factor. § $R_{\rm Cullis}$ is the Cullis R for centric reflections $= \sum \big||F_{\rm der} \pm F_{\rm nat}| - |F_{\rm H}|\big| / \sum |F_{\rm der} \pm F_{\rm nat}|$, where $F_{\rm nat}$, $F_{\rm der}$ and $F_{\rm H}$ are the structure factors of the protein, derivative and the heavy atom, respectively. ¶ $F_{\rm H}/E$ is the ratio of the heavy-atom structure factor $F_{\rm H}$ to the residual lack of closure E, which equals the phasing power.

lead nitrate, were prepared by diffusion. Native and derivative data were collected from multiple crystals at 293 K using a San Diego Multiwire two-detector system (Hamlin, 1985) and the data were processed using the programs of Howard *et al.* (1985). The data statistics are summarized in Table 1. Six mercury sites and four lead sites were located by difference Patterson (Ten Eyck *et al.*, 1976) and refined using *HEAVY* (Terwilliger & Eisenberg, 1983). Given the asymmetric unit weight of 255 000 Da, the phasing power was insufficient to produce an interpretable electron-density map. The refined heavy-atom coordinates are provided in the supplementary material[1].

2.1.2. Molecular replacement. The structure was solved by molecular replacement using *MERLOT* (Fitzgerald, 1988) with data in the 4–8 Å resolution range. The search molecule consisted of an unrefined 2.7 Å model of *E. coli* tm-EF-Tu–MgGDP, which included one Mg^{2+}, GDP and residues 9–40, 60–258 and 260–393 (Jurnak *et al.*, 1989). The highest noncrystallographic symmetry axes in the self-rotation map were twofolds, tilted slightly from the crystallographic *y* axis. The cross-rotation revealed five orientations compatible with the noncrystallographic twofolds of the self-rotation analysis. The sixth orientation shared a pair of similar angles with an alternate solution and was eventually found using a finer grid sampling about each established Eulerian angle. The correct rotational and translational solutions for each of six molecules are summarized in the supplementary material[1]. Each solution was verified by cross-phasing the mercury-derivative sites with generated model phases. Using *RMINM* (Ward *et al.*, 1975), the refinement of the rotational and translational parameters of all six copies yielded an R value of 0.53.

2.1.3. Difference maps and refinement. For refinement, six sets of angular and translational parameters were applied to a refined 2.5 Å model of EF-Tu–MgGDP (Abel *et al.*, 1996), in which residues 40–58 had been omitted, and subjected to simulated annealing in *X-PLOR* (Brünger, 1992*a*,*b*) with manual model rebuilding using *O* (Jones *et al.*, 1991) and *OOPS* (Kleywegt & Jones, 1996). A random sample of 7% of reflections was set aside for cross-validation during refinement (Brünger, 1992*b*). Protein parameter and topology files were based on a survey of the Cambridge Structural Database by Engh & Huber (1991). After several refinement cycles of six independent copies of the model, the working R factor dropped to 26.7% for all reflections with F greater than 2.0σ. Suitable electron densities for tetracycline molecules were visible in both $2F_{\rm o} - F_{\rm c}$ and $F_{\rm o} - F_{\rm c}$ electron-density maps. A model of tetracycline using the TetR coordinates (PDB code 2trt; Hinrichs *et al.*, 1994; Kisker *et al.*, 1995) was placed in each copy. Parameter and topology files for tetracycline were generated with *XPLO2D* (Kleywegt, 1995). Angles, dihedrals and impropers were idealized based on Engh and Huber parameters. Group occupancy and individual restrained thermal factors of tetracycline molecules were alternately refined. To reduce the number of parameters, additional refinement was carried out with noncrystallographic symmetry (NCS) restraints applied domain by domain to all six copies. NCS restraints were not applied to the 31 amino acids that deviated significantly from noncrystallographic symmetry, including residues 8, 96–98, 140–148, 153, 219–224, 259–266, 281–282 and 393. Water molecules were assigned to top peaks in the $F_{\rm o} - F_{\rm c}$ map if the peaks satisfied reasonable distance and geometry criteria. Final rounds of positional and thermal factor refinement were carried out with *CNS* (Brünger *et al.*, 1998) using all reflections in the range 2.8–40.0 Å. An overall thermal factor correction and a bulk-solvent correction were applied.

2.2. $P4_32_12$ crystal form

2.2.1. Crystallization, data collection and processing. Tm-EF-Tu–MgGDP was crystallized as described in Jurnak (1985). A saturating amount of tetracycline powder was added directly to crystals in mother liquor. After 48 h, the crystals turned deep yellow. One crystal was swiped through 40% ethylene glycol and frozen in a liquid-nitrogen stream. Diffraction data were collected using an R-AXIS IV imaging plate equipped with a Rigaku rotating copper-anode X-ray generator. The crystal belonged to space group $P4_32_12$, with unit-cell parameters $a = 69.11$, $b = 69.11$, $c = 157.33$ Å and one complex per asymmetric unit. Data were processed using *MOSFLM* (Kabsch, 1993; Campbell, 1995), *SCALA* (Evans, 1997) and *TRUNCATE* (French & Wilson, 1978). The resulting data statistics are given in Table 1.

2.2.2. Molecular replacement. The tm-EF-Tu–MgGDP–tetracycline structure was phased by molecular replacement with *EPMR* (Kissinger *et al.*, 1999), using chain *A* residues 8–39, 59–260 and 264–393 from the $C222_1$ structure of tm-EF-Tu–MgGDP as a search model (Jurnak *et al.*, 1989). All reflections in the resolution range 4–10 Å were used in the molecular-replacement searches. The $C222_1$ form has high pseudo-$P4_32_12$ symmetry, so the search was straightforward.

[1] Supplementary material has been deposited in the IUCr electronic archive (Reference: SX5055). Services for accessing this material are described at the back of the journal.

Table 2
Crystal parameters, data collection and refinement.

Space group	$P2_1$	$P4_32_12$
Molecules of tm-EF-Tu–MgGDP per ASU	6	1
No. of non-H atoms per ASU	17463†	3068
Unique reflections	64651†	20748
Completeness of data		
All data (%)	91.6	92.5
Highest resolution shell (%)	80.3	60.5
Resolution range of highest shell (Å)	2.8–2.9	2.1–2.2
Refinement		
Resolution range (Å)	2.8–40.0	2.1–51.9
Reflections used in working data set	60050	19741
Reflections used in test data set	4601	1007
Ordered waters per ASU	244	160
R_{free}‡ (%)	22.3	23.4
R_{work}§ (%)	18.0	20.0
Bond r.m.s. deviation (Å)	0.02	0.01
Angle r.m.s. deviation (Å)	1.82	1.63
Mean thermal factors (Å^2)		
Protein	45.0	43.7
MgGDP	43.3	27.7
Tetracycline	48.2	34.8
Water	38.9	45.4

† Noncrystallographic symmetry-related molecules were restrained, as described in §2, to reduce the effective number of refinement parameters. ‡ R_{free} is the crystallographic refinement factor calculated for the reflections that were set aside for cross-validation and not used in refinement. § $R_{work} = \sum |F_o - F_c| / \sum |F_o|$ for the reflections used in the refinement calculations.

The top *EPMR* solution had $\theta_1, \theta_2, \theta_3$ cross-rotational angles of 201.5, 0.9 and 116.4° and x, y, z translations of 42.6, 1.1 and 80.2 Å, respectively. The *EPMR* result had a correlation coefficient of 68.9% and an R factor of 36.6%. The root-mean-square deviation between the initial $C222_1$ search model and the final refined $P4_32_12$ model was 0.48 Å.

2.2.3. Refinement. Crystallographic refinement was carried out in *CNS*. A random sample of 4.5% of the reflections was set aside for cross-validation during refinement. The initial rigid-body refinement considered each of the three domains of EF-Tu as a separate 'rigid body', followed by conjugate-gradient minimization. σ_A-Weighted electron-density maps (Read, 1986) were generated with *CNS* and manual model adjustment was performed with *O* (Jones *et al.*, 1990). Further model refinement included minimization, simulated annealing and temperature-factor refinement. A model of tetracycline from the $P2_1$ structure was placed in the electron density. The occupancies of the tetracycline molecules were determined by initializing their occupancies to 0.5 and their temperature factors to 40 Å^2. Subsequently, four refinement rounds of alternately applying grouped occupancy refinement and individual restrained temperature-factor refinement to the tetracyclines were carried out. The electron density of Cys81 was consistent with the modified amino acid *S*-hydroxycysteine (CSO); thus, Cys81 was replaced by CSO. Water molecules were added using *CNS* and evaluated using the 'water scrutinize' option of *MOLEMAN*. Based on those results, as well as distance criteria, three of the waters were assigned as sodium ions for further refinement. The electron density indicated alternate conformations of His11, Gln97, Arg123, Glu307 and His364. Alternate conformations were also included for residues adjacent to Gln97 in order to accommodate different main-chain and side-chain conformations of Gln97. Occupancies of alternate conformations were refined in *CNS* and normalized to sum to 100%. Density for an unknown solvent molecule was wedged between Arg269 and Glu272 of one protein copy and Phe261 and Arg262 of a symmetry-related molecule. Glyoxylic acid best fitted the density shape and was thus included in the model. Density for a small solvent molecule was also found on a symmetry axis between tetracycline and a symmetry-related copy. The density was tetrahedral and was thus modeled as a sulfate molecule. Because the sulfur lies on a special position, the O atoms from one copy of the SO_4^{2-} ion would superimpose on the symmetry-related O atoms of the second copy. To accommodate this, all of the atoms were assigned partial occupancy. Several rounds of refinement were performed with *REFMAC* (Murshudov *et al.*, 1997) to refine the position of this sulfate.

3. Results

3.1. Final models

Tm-EF-Tu–MgGDP is structured into three domains: domain 1, the guanine-nucleotide domain (residues 8–40 and 59–204), domain 2 (residues 205–298) and domain 3 (residues 299–393). The two peptide fragments of tm-EF-Tu–MgGDP, residues 8–44 and 59–393, are held together by noncovalent interactions and, with the exception of residues 40–44 and 260–263, retain the same conformation as found in the intact native EF-Tu–MgGDP structure (Abel *et al.*, 1996). The asymmetric unit of the final model of the $P2_1$ form consists of six copies each of the protein, GDP, tetracycline and Mg^{2+} as well as 244 water molecules (PDB code 2hdn). The occupancies of the six tetracycline molecules in the final model range from 0.56 to 0.77. The asymmetric unit of the final model of the $P4_32_12$ form consists of one copy each of protein, GDP, tetracycline, Mg^{2+}, SO_4^{2-} and glyoxylic acid as well as three Na^+ ions and 160 water molecules (PDB code 2hcj). Tetracycline refines to full occupancy in the $P4_32_12$ crystal. Neither model includes the flexible protein region 41–44 or the protein regions removed by trypsin treatment: 1–7 and 45–58. In Fig. 2, a tetracycline molecule is superimposed upon electron density from the final σ_A-weighted annealed omit $F_o - F_c$ map contoured at 2.1σ in space group $P4_32_12$. The final refinement statistics for both crystal forms are summarized in Table 2. The geometry of each model was evaluated using the *MolProbity* web server (Lovell *et al.*, 2003). Only two amino acids (0.5%), Pro82 and Ser221, fall outside the *MolProbity* allowed regions of φ and ψ values.

3.2. Antibiotic binding site

The tetracycline site in both crystal forms is located in domain 1, making major interactions with the functional groups in the GTPase active site of tm-EF-Tu–MgGDP. As shown in Figs. 1 and 2, the phenoldiketone moiety of tetracycline interacts directly with key atoms in the GTPase active site of EF-Tu. Tet O11 and Tet O12 coordinate to the Mg^{2+} and

Table 3
Mg^{2+} coordination and hydrogen bonds between tetracycline and tm-EF-Tu–MgGDP.

	Distance (Å)	
	$P2_1$	$P4_32_12$
Mg^{2+} coordination		
Tet O11	2.29	2.09
Tet O12	2.12	1.93
GDP O2β	2.24	2.06
Thr25 O$^{\gamma1}$	2.33	2.21
Wat 1 O	2.12	1.99
Wat 2 O	2.10	2.03
Hydrogen bonds		
GDP O2α···Tet O12a	2.62	2.70
Thr25 O$^{\gamma1}$···Tet O11	2.66	—
Thr25 O$^{\gamma1}$···Tet O12	—	2.69
Asp80 O$^{\delta2}$···Tet O10	3.26	3.27
Wat 3 O···Tet O1	—	2.52
Wat 3 O···Tet N21	2.69	—
Wat 4 O···Tet O6	—	3.04
Wat 4 O···Tet O1	—	3.03
Wat 5 O···Tet O6	—	2.94
Wat 6 O···Tet O21	—	2.65

Tet O12a (PDB atom label O1C) interacts with the α-phosphate group of GDP. Tetracycline also interacts with two amino acids, Thr25 and Asp80. Thr25 belongs to the conserved sequence of the α-phosphate-binding loop, (G/A)X_4GK(S/T) and Asp80 belongs to the Switch II trigger sequence, DX_2G, found in all GTPases and many ATPases (Bourne *et al.*, 1991). The hydrogen of Tet O10 fits into a small pocket lying within hydrogen-bonding distance of the carboxyl groups of Asp80. A proline, Pro82, that is invariant only in ribosomal GTPases stacks against ring *D* of tetracycline. Because the protein conformation is slightly different around Pro82 in each space group, there is a shift in the tetracycline that causes small changes in the intermolecular distances between tm-EF-Tu–MgGDP and tetracycline (listed in Table 3). Tetracycline replaces two well ordered water molecules found in the Mg^{2+} coordination in all EF-Tu structures (Abel *et al.*, 1996; Kjeldgaard & Nyborg, 1992; Berchtold *et al.*, 1993; Polekhina *et al.*, 1996). A slight distortion of the polar zwitterionic conformation of tetracycline (Stezowski, 1976) best fits the electron density and is used in the final model. In several ways, the binding site for tetracycline on tm-EF-Tu–MgGDP is reminiscent of the tetracycline-binding site on TetR (Hinrichs *et al.*, 1994; Kisker *et al.*, 1995). In the latter complex, Mg^{2+} coordinates to Tet O11 and Tet O12; similarly, a proline stacks against ring *D* of tetracycline. The remaining contacts differ substantially in detail, but are formed with amino acids that are highly conserved in the TetR classes (Hinrichs *et al.*, 1994).

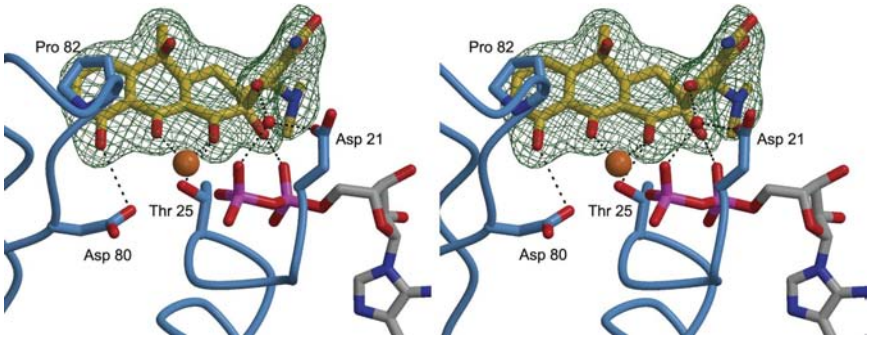

Figure 2
Stereoview of the superposition of tetracycline on a σ_A-weighted annealed omit $F_o - F_c$ electron-density map in which tetracycline has been omitted from the model phases in space group $P4_32_12$. The model is illustrated using the following colors: yellow for the C atoms and red for the O atoms of the tetracycline molecule, orange for Mg^{2+}, pink for the phosphates of GDP and blue ribbons for the protein backbone. The electron-density map is illustrated by green lines, which represent a contour level of 2.1σ. Hydrogen bonds are shown between key protein groups and tetracycline in dashed black lines. The figure was generated using *BobScript* (Esnouf, 1997) and *Raster3D* (Merritt & Bacon, 1997).

3.3. Intermolecular packing

3.3.1. $P2_1$ crystals. As shown in Fig. 3(*a*), the molecular unit of tm-EF-Tu–MgGDP–tetracycline in the $P2_1$ form is a dimer, which is stabilized by intermolecular contacts involving domains 1 and 2. In domain 1, the protein–protein interactions involve four antiparallel β-sheet hydrogen bonds between the pseudo-twofold-related residues 64 and 66′ as well as 66 and 64′, with the primes denoting noncrystallographically related residues. Hydrogen bonds are also formed between the side chain of Asn63 and the main chain of the pseudo-symmetry-related Glu68′ as well as between the main chain of Ile62 and the side chains of His66′ and Glu68′. In domain 2, residues 216, 259, 261, 262 and 287 form two electrostatic interactions and six hydrogen bonds with residues 216′, 261′, 262′ and 283′, ordering the Arg262–Leu264 loop, which is quite mobile in other EF-Tu–MgGDP structures. Additional van der Waals interactions between dimers, involving Ser219′–Ser221′ and Arg283′, appear to stabilize the flexible Ile220–Arg223 loop. The dimeric protein–protein contacts in domain 1 are similar to tm-EF-Tu–MgGDP dimers observed in other space groups, but the intermolecular antiparallel β-strand interactions in domain 1 are shifted by two amino acids and form fewer hydrogen bonds than in other dimers. The tetracycline rings are nearly parallel in the dimer unit, providing a significant hydrophobic environment, but the average ring distance of 7.0 Å is too far to denote a strong stacking interaction. The polar end of tetracycline, ring *A* and its substituents, are oriented toward the solvent but, given the limited data resolution, few water molecules can be placed with confidence in the region.

There are three sets of tm-EF-Tu–MgGDP–tetracycline dimers in the asymmetric unit of the $P2_1$ crystal. Each dimer is related to another pair by an oddly oriented pseudo-twofold axis but with minimal intermolecular contacts between the dimer sets. Although there are localized structural differences between the two protein copies within the dimer, each dimer of the tm-EF-Tu–MgGDP–tetracycline complex superimposes reasonably well upon other dimer copies. Moreover, the protein in the tetracycline complex superimposes well upon uncomplexed tm-EF-Tu–MgGDP and upon

intact EF-Tu–MgGDP, with C^{α} root-mean-square deviations of 0.48–0.82 and 0.49–1.76 Å, respectively. Thus, tetracycline does not appear to induce any significant changes in the protein conformation.

3.3.2. $P4_32_12$ crystals. As shown in Fig. 3(*b*), the closest packed molecules in the $P4_32_12$ form are related by the diagonal twofold axis. When one copy of the $P4_32_12$ dimer is superimposed upon a copy of the $P2_1$ dimer, the diagonal twofold axis is offset from the noncrystallographic twofold in the $P2_1$ dimer by 0.26 Å and a rotation of 29.6°. The protein–protein interactions in the $P4_32_12$ dimer involve six antiparallel β hydrogen bonds between the twofold-related residues 62 and 66′, and 64 and 64′, as well as 66 and 62′. Two hydrogen bonds are formed between the side chains of Asn63 and Ser65′ as well as those of Ser65 and Asn63′. Thus, the antiparallel β-strand interaction in the $P4_32_12$ pairs different residues compared with the $P2_1$ form and the difference is accompanied by a rotation of 60° of domains 2 and 3 relative to domains 2′ and 3′. The β-strand shift increases the buried surface area of the dimer in the $P4_32_12$ crystals from 2629 Å^2 to an average of 3205 Å^2 for the three $P2_1$ dimers (Jones & Thornton, 1996). There are only a few van der Waal contacts between domain 2 and domain 2′ in the region 261–272 and no hydrogen bonds nor electrostatic interactions in the $P4_32_12$ form compared with the $P2_1$ form. The shift also affects the relative position of the symmetry-related MgGDP and tetracycline molecules such that the symmetry-related antibiotic molecules are not stacked upon one another as they are in the $P2_1$ form.

3.4. Effect of trypsin modification

Trypsin modification of EF-Tu–MgGDP disorders residues 40–44 and 260–263 as well as removing residues 1–7 and 45–58. The latter 14 residues comprise the Switch I loop, whose conformation is regulated by the binding of MgGDP, MgGTP or EF-Ts (Abel & Jurnak, 1996; Kjeldgaard & Nyborg, 1992; Berchtold *et al.*, 1993; Polekhina *et al.*, 1996; Kawashima *et al.*, 1996). To determine whether tetracycline binding to tm-EF-Tu–MgGDP occurs only as a consequence of trypsin treatment, the tm-EF-Tu–MgGDP–tetracycline structure was superimposed upon other EF-Tu models. These included intact *E. coli* EF-Tu–MgGDP (Abel *et al.*, 1996), an *E. coli* homology model of *Thermus thermophilus* EF-Tu–MgGDPNP (Berchtold *et al.*, 1993), the *T. aquaticus* EF-Tu–MgGDPNP–yeast phenylalanyl-tRNA complex (Nissen *et al.*, 1995) and the *E. coli* EF-Tu–Ts–GDP complex (personal observation). The superposition results indicate that there are no clashes between tetracycline and the EF-Tu–Ts–GDP conformation. In the EF-Tu–MgGDP and EF-Tu–MgGTP conformations, tetracycline would be bound in a pocket formed in part by the flexible Switch I region. In the static structural states, the pocket is too small to accommodate tetracycline without minor clashes with Phe46, Asp50, Asn51 and Ala52 in the EF-Tu–MgGDP conformation and with Phe46, Asp50, Glu55, Gly59, Ile60, Thr61 and Asn63 in the EF-Tu–MgGTP conformation, whether phenylalanyl-tRNA is present or not. When tetracycline is placed into either the EF-Tu–MgGDP or the EF-Tu–MgGTP model and subjected to several rounds of energy-minimization, the Switch I region moves away sufficiently to permit tetracycline binding to the protein. The latter results suggest that tetracycline could bind to EF-Tu during a conformational change in the Switch I loop, with some amino acids shifting as much as 26 Å from the Switch I α-helix (residues 50–61) in the EF-Tu–MgGTP

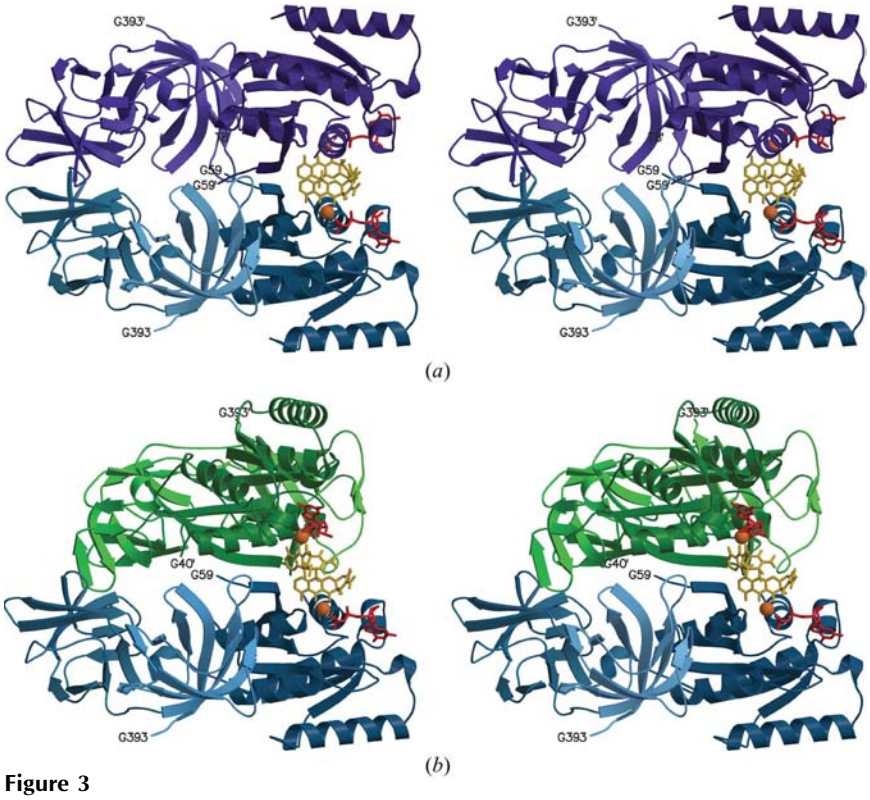

Figure 3
Comparison of the dimer units of tm-EF-Tu–MgGDP–tetracycline in the $P2_1$ and the $P4_32_12$ crystal forms. Stereo images of the dimers of tm-EF-Tu–MgGDP–tetracycline are shown for the $P2_1$ crystal form in (*a*) and for the $P4_32_12$ crystal form in (*b*). The bottom copy of each dimer pair for the two different space groups is shown in blue in the same orientation. In (*a*), the protein molecule in purple is related to the protein molecule in blue by a pseudo-twofold symmetry axis in space group $P2_1$. In (*b*), the protein molecule in green is related to the protein molecule in blue by a crystallographic twofold symmetry axis in space group $P4_32_12$. Within each molecule, the darkest hue is used for the N-terminal domain (domain 1) and the lightest hue for the C-terminal domain (domain 3). The GDP is represented by a red stick model, the Mg^{2+} ion by an orange sphere and the tetracycline by a yellow stick model. The stereo images illustrate the significant differences in the intermolecular interactions between the tm-EF-Tu–MgGDP pairs in the $P2_1$ and the $P4_32_12$ crystal forms. The views also depict the differences in the antiparallel β-strand interactions between the edge strand of each β-sheet in the nucleotide-binding domain of each protein copy. The images were created using *MolScript* (Kraulis, 1991) and *Raster3D* (Merritt & Bacon, 1997).

form to the Switch I β-ribbon (residues 50–61) in the EF-Tu–MgGDP form (Abel *et al.*, 1996; Polekhina *et al.*, 1996). Thus, the presence of tetracycline may affect the conversion rate from the EF-Tu–MgGTP to the EF-Tu–MgGDP conformation *in vitro* or *in vivo*, during which the Switch I interaction with the ribosome would be altered. No biochemical data are available to confirm or refute either possibility.

4. Discussion

4.1. Re-examination of the classical model of tetracycline inhibition

The fact that four distinctly different mechanisms for tetracycline resistance have been observed suggests that more than one mode of tetracycline inhibition may be operable in one or more different organisms. In the classical mode, tetracycline inhibits protein synthesis by preventing the binding of aminoacyl-tRNA to the A site of the ribosome (Schnappinger & Hillen, 1996; Chopra & Roberts, 2001). Yet the most striking feature of the present structural study is the molecular fit of tetracycline to a functionally critical region of EF-Tu. The fit is so perfect that it is unlikely to be fortuitous. The present result suggests that EF-Tu could be part of the tetracycline target during inhibition of protein synthesis. Indeed, several studies have implicated EF-Tu in the tetracycline-inhibition mechanism (Gordon, 1969; Lucas-Lenard *et al.*, 1969; Ravel *et al.*, 1969; Shorey *et al.*, 1969; Skoultchi *et al.*, 1970; Spirin *et al.*, 1976; Semenkov *et al.*, 1982). One study also demonstrates that tetracycline inhibits translocation, perhaps as a secondary effect (Werner *et al.*, 1975), implicating EF-G, an elongation factor that is homologous to EF-Tu in the tetracycline-binding region. Why then have the vast majority of studies over the last 35 years disavowed a role for any elongation factor? In raising the possibility of elongation-factor involvement once more, it is necessary to address the potential weaknesses in many experiments. Foremost are the technical difficulties associated with ribosomal preparations for *in vitro* assays. Not only is it challenging to prepare active ribosomes, but the initial studies (Hierowski, 1965; Suarez & Nathans, 1965; Day, 1966; Suzuka *et al.*, 1966) as well as many recent ones have also used ribosomes washed with 0.5 *M* salt or lower. It is now known that only salt washes greater than 1.0 *M* effectively remove contaminating EF-Tu and EF-G (Hamel *et al.*, 1972; Jelenc, 1980). Thus, the possibility exists that the interpretations of many *in vitro* ribosomal studies with tetracycline are invalidated by EF-Tu or EF-G contaminants.

A second potential problem is the Mg^{2+} concentration used in ribosomal assays. At Mg^{2+} levels of 10 m*M* or lower, the standard assay requires EF-Tu–MgGTP for proper aminoacyl-tRNA placement. At Mg^{2+} concentrations of 20 m*M* or higher, aminoacyl-tRNA is placed in the A site in the absence of EF-Tu–MgGTP. Indeed, tetracycline inhibition of the non-enzymatic EF-Tu-independent *in vitro* ribosomal assay is frequently considered as proof that elongation factors play no role. Unfortunately, most non-enzymatic assays use Mg^{2+} concentrations of 11–13 m*M* and do not account for the 2.7 mM^{-1} affinity of free tetracycline for Mg^{2+} (Degenkolb *et al.*, 1991). It is quite possible that in many of the studies tetracycline appears to inhibit the non-enzymatic assays because the available Mg^{2+} concentration drops by binding to tetracycline to levels that require participation by EF-Tu–MgGTP. Semenkov and colleagues have carried out *in vitro* ribosomal assays at appropriate Mg^{2+} concentrations of 10 and 20 m*M* and observe a distinct difference in the mode of tetracycline inhibition between EF-Tu-dependent and EF-Tu-independent assays (Semenkov *et al.*, 1982). Under EF-Tu-independent conditions, aminoacyl-tRNA placement in the A site is reversible and weak in the presence of tetracycline. In contrast, under EF-Tu-dependent conditions tetracycline slows the kinetics of aminoacyl-tRNA binding but does not affect the final stoichiometry or relative affinity of aminoacyl-tRNA binding for the A site. These experiments provide the strongest biochemical evidence for some type of EF-Tu participation in tetracycline inhibition of protein synthesis. Taken together, the points raised do not necessarily invalidate any prior conclusions, but simply call into question whether the widely accepted mode of tetracycline inhibition is complete.

4.2. Tetracycline as a lead compound in rational drug-design studies

A significant finding of the present study is the molecular fit between the phenoldiketone moiety of tetracycline and the GTPase active site of EF-Tu shown in Fig. 2. Many pharmacological agents share chemical similarities with the O10-C10-C10a-C11-O11 grouping in tetracycline and this chemical moiety could potentially bind to an Mg^{2+} ion and the invariant amino acids found in all GTPases and the P-loop-containing ATPases. The relevant invariant amino acids are analogous to the 18-Gly-$(Xxx)_4$-Gly-Lys-Thr-25 sequence in the phosphate-binding loop of EF-Tu as well as the 80-Asp-$(Xxx)_2$-Gly-83 sequence, which controls the conformational changes germane to GTP or ATP hydrolysis in the Switch II region. Whether tetracycline binds to any GTPase or ATPase would depend upon the local sequence and structural environment of the nucleotide pocket. However, it is not difficult to envision that phenoldiketone moiety of tetracycline could be used as an initial lead compound in combinatorial chemical experiments or in the rational design of new agents to fit specifically into the nucleotide pockets of selected GTPase or ATPase targets. The use of functionally critical amino acids in the binding of tetracycline has the advantage of blocking simple resistance mechanisms involving site-specific amino-acid mutations, which reduce the antibiotic affinity, because such mutations would also inactivate the protein.

5. Conclusions

The structure of the tm-EF-Tu–MgGDP–tetracycline complex reveals a precise molecular fit between the pharmacologically active phenoldiketone moiety of tetracycline and the GTPase active site of EF-Tu. This finding, together with a review of

literature reports on the mode of tetracycline action and resistance, suggests that EF-Tu may have an *in vivo* role in tetracycline inhibition of protein synthesis. Such information may be useful in the design of tetracycline derivatives that are more effective as well as circumvent known antibiotic resistance mechanisms. Should further studies prove that EF-Tu does not participate in tetracycline inhibition, the present results nevertheless suggest that tetracycline is a viable lead compound in the design of newer pharmaceutical agents targeted against specific GTPases or ATPases. In such an endeavor, the atomic coordinates of the tm-EF-Tu–MgGDP–tetracycline complex should be invaluable.

The authors thank Xuong Nguyen-Huu for use of the area-detector facility at UC San Diego, the San Diego Supercomputer Center and the Public Health Service (award GM26895 to FJ) for support of the research.

References

Abel, K. & Jurnak, F. (1996). *Structure*, **4**, 229–238.
Abel, K., Yoder, M. D., Hilgenfeld, R. & Jurnak, F. (1996). *Structure*, **4**, 1153–1159.
Berchtold, H., Reshetnikova, L., Reiser, C. O., Schirmer, N. K., Sprinzl, M. & Hilgenfeld, R. (1993). *Nature (London)*, **365**, 126–132.
Bourne, H. R., Sanders, D. A. & McCormick, F. (1991). *Nature (London)*, **349**, 117–127.
Brodersen, D., Clemons, W. M., Carter, A. P., Morgan-Warren, R. J., Wimberly, B. T. & Ramakrishnan, V. (2000). *Cell*, **103**, 1143–1154.
Brown, J. R. & Ireland, D. S. (1978). *Adv. Pharmacol. Chemother.* **15**, 161–202.
Brünger, A. T. (1992*a*). *X-PLOR Version* 3.1. *A System for X-ray Crystallography and NMR*. Yale University, New Haven, CT, USA.
Brünger, A. T. (1992*b*). *Nature (London)*, **355**, 472–474.
Brünger, A. T., Adams, P. D., Clore, G. M., DeLano, W. L., Gros, P., Grosse-Kunstleve, R. W., Jiang, J.-S., Kuszewski, J., Nilges, M., Pannu, N. S., Read, R. J., Rice, L. M., Simonson, T. & Warren, G. L. (1998). *Acta Cryst.* D**54**, 905–921.
Buck, M. A. & Cooperman, B. S. (1990). *Biochemistry*, **29**, 5374–5379.
Campbell, J. W. (1995). *J. Appl. Cryst.* **28**, 236–242.
Chopra, I. & Roberts, M. (2001). *Microbiol. Mol. Rev.* **65**, 232–260.
Connamacher, R. H. & Mandel, H. G. (1968). *Biochem. Biophys. Acta*, **166**, 475–486.
Day, L. E. (1966). *J. Bacteriol.* **91**, 1917–1923.
Degenkolb, J., Takahashi, M., Ellestad, G. A. & Hillen, W. (1991). *Antimicrob. Agents Chemother.* **35**, 1591–1595.
Engh, R. & Huber, R. (1991). *Acta Cryst.* A**47**, 392–400.
Epe, B. & Woolley, P. (1984). *EMBO J.* **3**, 121–126.
Esnouf, R. M. (1997). *J. Mol. Graph.* **15**, 132–134.
Evans, P. R. (1997). *Jnt CCP4/ESF–EACBM Newsl. Protein Crystallogr.* **33**, 22–24.
Fitzgerald, P. M. D. (1988). *J. Appl. Cryst.* **21**, 273–278.
French, G. S. & Wilson, K. S. (1978). *Acta Cryst.* A**34**, 517–525.
Goldman, R. A., Hasan, T., Hall, C. C., Strycharz, W. A. & Cooperman, B. S. (1983). *Biochemistry*, **22**, 359–368.
Gordon, J. (1969). *J. Biol. Chem.* **242**, 5564–5571.
Hamel, E., Koka, M. & Nakamoto, T. (1972). *J. Biol. Chem.* **247**, 805–814.
Hamlin, R. (1985). *Methods Enzymol.* **114**, 416–452.
Hierowski, M. (1965). *Proc. Natl Acad. Sci. USA*, **53**, 594–599.
Hinrichs, W., Kisker, C., Duvel, M., Muller, A., Tovar, K., Hillen, W. & Saenger, W. (1994). *Science*, **264**, 418–420.
Howard, A. J., Nielsen, C. & Xuong, N.-H. (1985). *Methods Enzymol.* **114**, 452–472.
Jelenc, P. C. (1980). *Anal. Biochem.* **105**, 369–374.
Jones, S. & Thornton, J. M. (1996). *Proc. Natl Acad. Sci. USA*, **93**, 13–20.
Jones, T. A., Bergdoll, M. & Kjeldgaard, M. (1990). *Crystallographic and Modeling Methods in Molecular Design*, edited by C. Bugg & S. Ealick, pp. 189–195. New York: Springer–Verlag.
Jones, T. A., Zou, J.-Y., Cowan, S. W. & Kjeldgaard, M. (1991). *Acta Cryst.* A**47**, 110–119.
Jurnak, F. (1985). *J. Mol. Biol.* **185**, 215–217.
Jurnak, F., Nelson, M., Yoder, M., Heffron, S. & Mui, S. (1989). *The Guanine-Nucleotide Binding Proteins*, edited by L. Bosch, B. Kraal & A. Parmeggiani, pp. 15–25. New York: Plenum Press.
Kabsch, W. (1993). *J. Appl. Cryst.* **26**, 795–800.
Kawashima, T., Berthet-Columinas, C., Wulff, M., Cusack, S. & Leberman, R. (1996). *Nature (London)*, **379**, 511–518.
Kisker, C., Hinrichs, W., Tovar, K., Hillen, W. & Saenger, W. (1995). *J. Mol. Biol.* **247**, 260–280.
Kissinger, C. R., Gehlhaar, D. K. & Fogel, D. B. (1999). *Acta Cryst.* D**55**, 484–491.
Kjeldgaard, M. & Nyborg, J. (1992). *J. Mol. Biol.* **223**, 721–742.
Kleywegt, G. J. (1995). *Jnt CCP4/ESF–EACBM Newsl. Protein Crystallogr.* **31**, 45–50.
Kleywegt, G. J. & Jones, T. A. (1996). *Acta Cryst.* D**52**, 826–828.
Kraulis, P. J. (1991). *J. Appl. Cryst.* **24**, 946–950.
Maxwell, H. (1968). *Mol. Pharmacol.* **4**, 25–37.
Merritt, E. A. & Bacon, D. J. (1997). *Methods Enzymol.* **277**, 505–524.
Lovell, S. C., Davis, I. W., Arendall, W. B., de Bakker, P. I. W., Word, J. M., Prisant, M. G., Richardson, J. S. & Richardson, D. C. (2003). *Proteins*, **50**, 437–450.
Lucas-Lenard, J., Tao, P. & Haenni, A. L. (1969). *Cold Spring Harb. Symp. Quant. Biol.* **34**, 455–462.
Moazed, D. & Noller, H. F. (1987). *Nature (London)*, **327**, 389–394.
Mui, S., Delaria, K. & Jurnak, F. (1990). *J. Mol. Biol.* **212**, 445–447.
Murshudov, G. N., Vagin, A. A. & Dodson, E. J. (1997). *Acta Cryst.* D**53**, 240–255.
Nissen, P., Kjeldgaard, M., Thirup, S., Polekhina, G., Reshetnikova, L., Clark, B. F. & Nyborg, J. (1995). *Science*, **270**, 1464–1472.
Noah, J. W., Dolan, M. A., Babin, P. & Wollenzien, P. (1999). *J. Biol. Chem.* **274**, 16576–16581.
Nonaka, L., Connell, S. R. & Taylor, D. E. (2005). *J. Bacteriol.* **187**, 3708–3712.
Oehler, R., Polacek, N., Steiner, G. & Barta, A. (1997). *Nucleic Acids Res.* **25**, 1219–1224.
Orth, P., Saenger, W. & Hinrichs, W. (1999). *Biochemistry*, **38**, 191–198.
Pioletti, M., Schlünzen, F., Harms, J., Zarivach, R., Glühmann, M., Avila, H., Bashan, A., Bartels, H., Auerbach, T., Jacobi, C., Hartsch, T., Yonath, A. & Franceschi, F. (2001). *EMBO J.* **20**, 1829–1839.
Polekhina, G., Thirup, S., Kjeldgaard, M., Nissen, P., Lippmann, C. & Nyborg, J. (1996). *Structure*, **4**, 1141–1151.
Ravel, J. M., Shorey, R. L., Garner, C. W., Dawkins, R. C. & Shive, W. (1969). *Cold Spring Harb. Symp. Quant. Biol.* **34**, 321–330.
Read, R. J. (1986). *Acta Cryst.* A**42**, 140–149.
Rogalski, W. (1985). *Handbook of Experimental Pharmacology*, edited by J. J. Hlavka & J. H. Boothe, Vol. 78, pp. 179–316. Berlin: Springer–Verlag.
Ross, J. I., Eady, E. A., Cove, J. H. & Cunliffe, W. J. (1998). *Antimicrob. Agents Chemother.* **42**, 1702–1705.
Schnappinger, D. & Hillen, W. (1996). *Arch. Microbiol.* **165**, 359–369.
Semenkov, Y. P., Makarov, E. M., Makhno, V. I. & Kirillov, S. V. (1982). *FEBS Lett.* **144**, 125–129.
Shorey, R. L., Ravel, J. M., Garner, C. W. & Shive, W. (1969). *J. Biol. Chem.* **244**, 4555–4564.
Skoultchi, A., Ono, Y., Waterson, J. & Lengyel, P. (1970). *Biochemistry*, **9**, 508–514.

Spirin, A. S., Kostiashkina, O. E. & Jonak, J. (1976). *J. Mol. Biol.* **101**, 553–562.
Stezowski, J. J. (1976). *J. Am. Chem. Soc.* **98**, 6012–6018.
Suarez, G. & Nathans, D. (1965). *Biochem. Biophys. Res. Commun.* **18**, 743–750.
Suzuka, I., Kaji, H. & Kaji, A. (1966). *Proc. Natl Acad. Sci. USA*, **55**, 1483–1490.
Ten Eyck, L., Weaver, L. A. & Matthews, B. W. (1976). *Acta Cryst.* A**32**, 349–355.
Terwilliger, T. C. & Eisenberg, D. E. (1983). *Acta Cryst.* A**39**, 813–817.
Ward, K. B., Wishner, B. C., Lattman, E. E. & Love, W. E. (1975). *J. Mol. Biol.* **98**, 161–177.
Werner, R., Kollak, A., Nierhaus, D., Schreiner, G. & Nierhaus, K. H. (1975). *Topics in Infectious Diseases*, edited by J. Drews & F. G. Hahn, Vol. 1, pp. 217–234. Berlin: Springer–Verlag.
Williams, G. & Smith, I. (1979). *Mol. Gen. Genet.* **177**, 23–29.